

## Temperature dependent transport behavior of n -InN nanodot / p -Si heterojunction structures

Thirumaleshwara N. Bhat, Basanta Roul, Mohana K. Rajpalke, Mahesh Kumar, S. B. Krupanidhi, and Neeraj Sinha

Citation: [Applied Physics Letters](#) **97**, 202107 (2010); doi: 10.1063/1.3517489

View online: <http://dx.doi.org/10.1063/1.3517489>

View Table of Contents: <http://scitation.aip.org/content/aip/journal/apl/97/20?ver=pdfcov>

Published by the [AIP Publishing](#)

---

### Articles you may be interested in

[Effect of band offset on carrier transport and infrared detection in InP quantum dots/Si nano-heterojunction grown by metalorganic chemical vapor deposition technique](#)

*J. Appl. Phys.* **115**, 203719 (2014); 10.1063/1.4880738

[Growth mechanism and microstructure of low defect density InN \(0001\) In-face thin films on Si \(111\) substrates](#)

*J. Appl. Phys.* **114**, 163519 (2013); 10.1063/1.4827396

[Multiple-level threshold switching behavior of In<sub>2</sub>Se<sub>3</sub> confined in a nanostructured silicon substrate](#)

*Appl. Phys. Lett.* **97**, 092114 (2010); 10.1063/1.3486122

[Accommodation mechanism of InN nanocolumns grown on Si\(111\) substrates by molecular beam epitaxy](#)

*Appl. Phys. Lett.* **91**, 021902 (2007); 10.1063/1.2756293

[Growth of high-quality GaAs on Ge/Si 1 - x Ge x on nanostructured silicon substrates](#)

*Appl. Phys. Lett.* **88**, 251909 (2006); 10.1063/1.2214145

---

The advertisement features a dark background with a grid pattern. On the left, there is a 3D cutaway illustration of a mechanical part with a red and yellow color gradient. The text 'Over 600 Multiphysics Simulation Projects' is prominently displayed in white and blue. A blue button with the text 'VIEW NOW >>' is located to the right of the main text. The COMSOL logo is in the bottom right corner.

Over **600** Multiphysics Simulation Projects

[VIEW NOW >>](#)

COMSOL

## Temperature dependent transport behavior of *n*-InN nanodot/*p*-Si heterojunction structures

Thirumaleshwara N. Bhat,<sup>1</sup> Basanta Roul,<sup>1,2</sup> Mohana K. Rajpalke,<sup>1</sup> Mahesh Kumar,<sup>1,2</sup> S. B. Krupanidhi,<sup>1,a)</sup> and Neeraj Sinha<sup>3</sup>

<sup>1</sup>Materials Research Centre, Indian Institute of Science, Bangalore 560012, India

<sup>2</sup>Central Research Laboratory, Bharat Electronics, Bangalore 560013, India

<sup>3</sup>Office of Principal Scientific Advisor, Government of India, New Delhi 110011, India

(Received 5 August 2010; accepted 28 October 2010; published online 18 November 2010)

The present work explores the temperature dependent transport behavior of *n*-InN nanodot/*p*-Si(100) heterojunction diodes. InN nanodot (ND) structures were grown on a 20 nm InN buffer layer on *p*-Si(100) substrates. These dots were found to be single crystalline and grown along [001] direction. The junction between these two materials exhibits a strong rectifying behavior at low temperatures. The average barrier height (BH) was determined to be 0.7 eV from current-voltage-temperature, capacitance-voltage, and flat band considerations. The band offsets derived from built-in potential were found to be  $\Delta E_C=1.8$  eV and  $\Delta E_V=1.3$  eV and are in close agreement with Anderson's model. © 2010 American Institute of Physics. [doi:10.1063/1.3517489]

InN is a promising material among the III-nitride semiconductors due to its narrow bandgap energy ( $\sim 0.65$  eV) and high carrier mobility ( $\sim 3500$  cm<sup>2</sup> V<sup>-1</sup> s<sup>-1</sup>). Although InN exhibits metallic behavior due to large background electron concentration,<sup>1</sup> several studies on GaN heterojunctions are reported earlier.<sup>1,2</sup> However, no report is evident on the temperature dependent heterojunction behavior of InN nanostructures grown on Si. Since silicon is the most sought semiconductor material, it is very important to understand the transport mechanism of InN nanostructure based devices and their behavior at different temperatures prior to their adoption in the fabrication of optoelectronic devices. In the present study, we examine the results obtained from the heterojunction transport behavior of InN nanodot (ND) based structures at different temperatures.

The fabrication of the InN NDs on *p*-Si(100) was carried out by plasma assisted molecular beam epitaxy (PAMBE) system. The deposition of InN consists of a two step growth method. The initial low temperature buffer layer was deposited at 410 °C for 10 min. Further, the substrate temperature was raised to 500 °C to fabricate the nanodots. The duration of ND growth was kept for 60 min. The general set of growth conditions includes indium beam equivalent pressure, nitrogen flow rate, and rf-plasma power, which were kept at  $2 \times 10^{-7}$  mbar, 0.5 SCCM (SCCM denotes cubic centimeter per minute at STP), and 350 W, respectively. The structural evaluation of the as-grown NDs was carried out by the x-ray diffraction, scanning electron microscopy (SEM), and transmission electron microscopy (TEM). The aluminum contacts were fabricated by thermal evaporation. The adequate Ohmic nature of the contacts to InN and Si was verified. The device transport characteristics were studied at various temperatures using the probe station attached with the KEITHLEY-236 source measure unit and an LCZ-3330 meter.

Figure 1(a) shows a typical field emission scanning electron microscopy (FESEM) image of InN NDs and illustrates that the as-grown NDs are vertically aligned and uniformly grown over the entire substrate. The average height and di-

ameter of these dots were found to be 100 nm. The x-ray diffraction studies on InN NDs exhibited a peak at  $2\theta = 31.37^\circ$  illustrating the (0002) reflection of wurtzite InN. Figures 1(b)–1(d) represent typical transmission electron micrographs, selected area electron diffraction (SAED), and high resolution TEM (HRTEM) images of InN NDs, respectively. In particular, the HRTEM [Fig. 1(d)] shows one of the corner edges of a ND. From the TEM and SEM images, one can conclude that the shape of the NDs corresponds to a perfect hexagon in the film plane and a truncated pyramid in the vertical direction with very clear crystallographic facets of hexagonal structure. It can be described more accurately as a truncated pyramid with hexagonal base with a base diameter few times larger than the height. Such growth behavior is in agreement with that reported earlier.<sup>3</sup> The SAED pattern is indexed to the reflections of hexagonal InN crystal along the [001] direction. The interplanar spacing, as observed from the fringe pattern of the HRTEM image, is 0.308 nm, which corresponds to the (100) lattice spacing of InN.<sup>4</sup> These data clearly demonstrate that the as-grown NDs are fairly single crystalline, and are crystallized hexagonally along the [001] direction with uniform geometry.

Studies of the current-voltage characteristics of the fabricated *n*-InN ND/*p*-Si heterostructures revealed the presence of good rectifying characteristics. The carrier densities of InN and Si were found to be  $6.5 \times 10^{18}$  and  $2 \times 10^{18}$  cm<sup>-3</sup>, respectively, measured by Hall measurements. However, the incidental doping in InN NDs was unintentional. Figure 2(a) shows the temperature dependent *I*-*V* characteristics of the junction in the temperature range of 173–473 K. An excellent rectifying behavior was observed at lower temperatures with an on/off ratio of 206 at 10 V. The deterioration observed in the rectifying nature at high temperature may be due to thermally generated carrier tunneling. Slight reduction in the forward current at higher voltages and a temperature of 473 K was observed. This behavior can be ascribed to pronounced diffusion current at high bias voltage, arising from the linear reduction in the barrier for electron and hole diffusion current. From the Einstein's relation,  $D = (kT/q)\mu$ , the diffusion current is strongly dependent on the

<sup>a)</sup>Electronic mail: sbk@mrc.iisc.ernet.in.

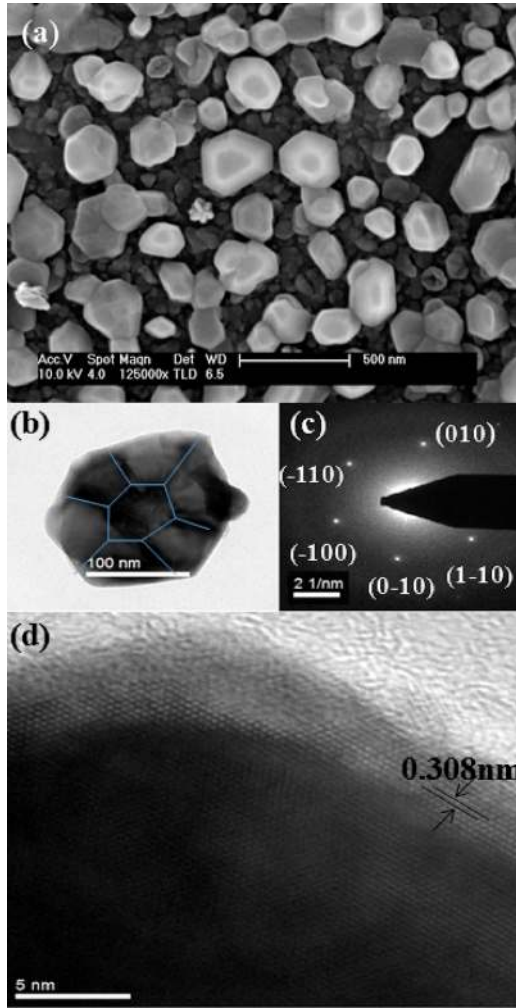


FIG. 1. (Color online) (a) FESEM image of the InN NDs. (b) Typical TEM image of a ND showing the hexagonal facets. (c) SAED pattern taken along the [001] direction. (d) HRTEM of the corner edge of a ND.

mobility of the carriers. Thakur *et al.*<sup>5</sup> observed for InN that mobility stays almost constant over a large temperature range due to a negligible thermal activation. However, at higher temperatures, the phonon population increases, resulting in a reduction in the mobility.

The  $I$ - $V$  curves were fitted by using the single carrier thermionic emission expression,

$$I = I_s \left[ \exp\left(\frac{qV}{\eta kT}\right) - 1 \right] \quad \text{where } I_s = AA^*T^2 \exp\left(-\frac{\phi_b}{kT}\right). \quad (1)$$

The zero bias (ZB) barrier heights (BHs) are evaluated at each temperature, variation of ZB BH ( $\phi_b$ ) and ideality factor  $\eta$  with temperature is shown in Fig. 2(b). A dependence of  $\phi_b$  and  $\eta$  on the temperature is clearly observed and is attributed to the inhomogeneity at the interface.<sup>6</sup> A variation of the  $\phi_b$  as a function of  $\eta$  with a linear correlation was also observed. Such behavior can be associated with a nonuniform Schottky interface.<sup>6</sup> Since the BH depends on the electric field across the interface and consequently on the applied voltage, it is necessary to consider the standard field conditions. The electric field is zero across the interface under flat band (FB) conditions. The FB BH is given by

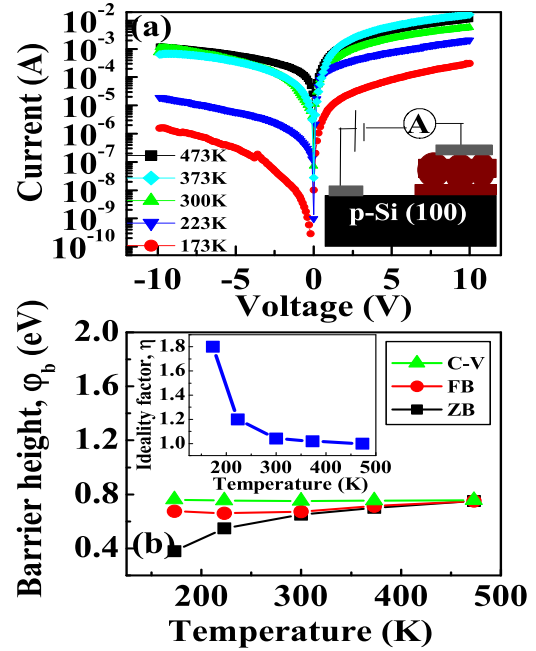


FIG. 2. (Color online) (a) Current vs voltage plots of the InN ND/ $p$ -Si diode at different temperatures. The inset shows a schematic diagram of the device and measurement method. (b) Variation of ZB, FB, and  $C$ - $V$  barrier heights and ideality factor with temperature.

$$\phi_{bf} = \eta\phi_b - (\eta - 1)(kT/e)\ln(N_V/N_A),$$

where  $N_V = 1.04 \times 10^{19} \text{ cm}^{-3}$  at room temperature is the effective density of states of the valence band of  $p$ -Si. The  $\phi_{bf}$  values are plotted in Fig. 2(b). The Richardson's constant of  $54 \text{ A cm}^{-2} \text{ K}^{-2}$  and barrier height of 0.7 eV were obtained from the “modified” Richardson's plot, which is in close agreement with the effective Richardson's constant of  $p$ -Si ( $\sim 32 \text{ A cm}^{-2} \text{ K}^{-2}$ ).

Figure 3(a) shows the characteristic of  $C$ - $V$  measurements performed on the heterojunctions at 100 kHz in the temperature range of 173–473 K. For a Schottky diode,  $C$ - $V$  relationship can be expressed as

$$1/C^2 = [(2/\epsilon)eN_A A^2)(V_{bi} - V - kT/e)],$$

where  $\epsilon$  is the permittivity of silicon,  $V_{bi}$  is the built-in potential, and  $N_A$  is the doping density of Si. The built-in potential  $V_{bi}$  can be determined by linearly extrapolating the  $C^{-2}$ - $V$  curve to the voltage axis. Therefore, the  $C$ - $V$  BH is  $\phi_b = V_{bi} + (kT/e)\ln(N_V/N_A)$ . The  $\phi_{b(C-V)}$  values obtained are plotted in Fig. 2(b), and it can be seen that the FB BH is invariably larger than the ZB BH at low temperature. Further, the FB BH mirrors  $C$ - $V$  BH with slight reduction in BH values at low temperature. This is possibly due to the tunneling and leakage through the dislocations and other defects resulting in high values of ideality factor ( $\eta > 1$ ), which increases with decreasing temperature. In contrast to the case of ZB, the field is zero under flat band conditions, which eliminates the tunneling and image force lowering, and removes the influence of lateral inhomogeneities. For these reasons,  $I$ - $V$  measurements would yield unreliable results in barrier height and band offset determinations. Hence, the band offsets of the present heterostructures were determined using built-in voltage of  $C$ - $V$  analysis for the room temperature by following the relations<sup>7</sup>

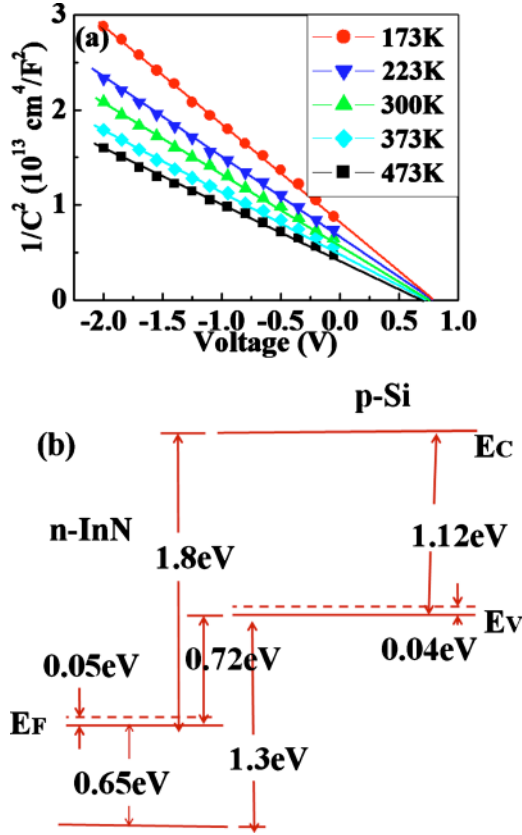


FIG. 3. (Color online) (a) Reverse bias capacitance-voltage characteristics of InN ND/*p*-Si diode at different temperatures. (b) Flat band energy band diagram for InN/*p*-Si heterostructures.

$$\Delta E_C = E_g \text{Si} + [(E_C - E_F) \text{InN} + V_{\text{bi}} - (E_F - E_V) \text{Si}]$$

and

$$\Delta E_V = E_g \text{InN} + [(E_C - E_F) \text{InN} + V_{\text{bi}} - (E_F - E_V) \text{Si}],$$

where  $E_C - E_F = (kT/e) \ln(N_C/N_D)$  and  $E_F - E_V = (kT/e) \ln(N_V/N_A)$ . The band offsets for InN/*p*-Si at flat

band conditions are shown in Fig. 3(b). The band offset results showed a good agreement with Anderson's model, i.e.,

$$\Delta E_C = X_{\text{InN}} - X_{\text{Si}} \quad \text{and} \quad \Delta E_V = \Delta E_g - \Delta E_C,$$

where  $X_{\text{InN}} = 5.8$  eV and  $X_{\text{Si}} = 4.05$  eV are the electron affinities of InN and Si, respectively. The nonsymmetry in the band offsets would tend to make the potential barrier less for holes than electrons. Hence, the single carrier thermionic emission relation has been chosen in *I*-*V* data interpretation.

In conclusion, the Si heterojunction diodes were fabricated by depositing InN NDs using PAMBE, the as-grown ND structures are single crystalline and grown along the [001] direction. The transport behavior of the diodes was studied at various bias voltages and temperatures. The temperature dependent ZB BH and ideality factors of the forward *I*-*V* data are observed, while it was governed through the modified Richardson's plot. The modified Richardson's constant and barrier height were found to be  $54 \text{ A cm}^{-2} \text{ K}^{-2}$  and 0.7 eV, respectively. The difference in FB BH and *C*-*V* BH and the deviation of ideality factor from unity indicate the presence of inhomogeneities at the interface. The average Schottky BHs were determined to be 0.7 eV by *C*-*V* and flat band considerations. The band offsets derived from *C*-*V* measurements were found to be  $\Delta E_C = 1.8$  eV and  $\Delta E_V = 1.3$  eV, which are in close agreement with Anderson's model.

<sup>1</sup>N. C. Chen, P. H. Chang, Y. N. Wang, H. C. Peng, W. C. Lien, C. F. Shih, C. Chang, and G. M. Wu, *Appl. Phys. Lett.* **87**, 212111 (2005).

<sup>2</sup>K. Wang, C. Lian, N. Su, and D. Jena, *Appl. Phys. Lett.* **91**, 232117 (2007).

<sup>3</sup>F. Demangeot, J. Frandon, C. Pinquier, M. Caumont, O. Briot, B. Maleyre, S. Clur-Ruffenach, and B. Gil, *Phys. Rev. B* **68**, 245308 (2003).

<sup>4</sup>C. H. Liang, L. C. Chen, J. S. Hwang, K. H. Chen, Y. T. Hung, and Y. F. Chen, *Appl. Phys. Lett.* **81**, 22 (2002).

<sup>5</sup>J. S. Thakur, R. Naik, V. M. Naik, D. Haddad, G. W. Auner, H. Lu, and W. J. Schaff, *J. Appl. Phys.* **99**, 023504 (2006).

<sup>6</sup>F. Iucolano, *J. Appl. Phys.* **102**, 113701 (2007).

<sup>7</sup>J. T. Torvik, M. Leksono, J. I. Pankove, B. V. Zeghbroeck, H. M. Ng, and T. D. Moustakas, *Appl. Phys. Lett.* **72**, 1371 (1998).